Mechanics & Industry **20**, 627 (2019)
© AFM, EDP Sciences 2019
https://doi.org/10.1051/meca/2019073

Mechanics & Industry

Available online at:
www.mechanics-industry.org

Regular Article

1D gas dynamic code for performance prediction of one turbocharger radial turbine with different finite difference schemes

Ahmed Ketata*, Zied Driss, and Mohamed Salah Abid

Laboratory of Electro-Mechanic Systems, National School of Engineers of Sfax, University of Sfax, B.P. 1173, km 3.5 Road Soukra, 3038 Sfax, Tunisia

Received: 30 November 2017 / Accepted: 11 October 2019

Abstract. The turbine, a key component of a turbocharger, is usually characterized by steady flow solutions. This method seems to be physically unrealistic as the fluid flow within a turbine is strongly unsteady due to the pulsating nature of the flow in the exhaust manifold of a reciprocating engine. This paper presents a new 1D gas dynamic code, written in the FORTRAN language, to characterize a radial turbine of one turbocharger embedded to a small gasoline engine. This code presents the novelty of meanline-1D coupling and the feature of numerical schemes choice. In this study, the turbocharger turbine is simulated with six different finite difference schemes. The computed distribution of the downstream mass flow rate, from the different cases, is compared to test data in order to choose the most suitable scheme. Test data are gathered from a developed test facility. Based on the computed results, unsteady performance of the turbine has been computed and discussed for the different schemes at two engine frequencies of 50 and 83.33 Hz. The results showed a significant impact of the numerical scheme on the 1D prediction of the turbine performance. Results indicated that the MR2LW finite-difference scheme has led to the minimum deviation of the numerical results to test data compared to the other considered schemes.

Keywords: Turbocharging / internal combustion engine / turbine / CFD / 1D modeling

1 Introduction

Stringent emission regulations are pushing more and more manufacturers to produce green engines. Downsizing technics are among alternative approach to reduce the emissions of internal combustion engines (ICE). This method requires the embedding of advanced technological components such as multistage and variable geometry turbochargers, Exhaust Gas Recirculation (EGR), direct injection, Diesel Particulate Filter (DPF), and catalytic converters. It is widely understood that turbocharging is a beneficial system, applied in both gasoline and diesel engines, for power improvement and exhaust emissions reducing. Moreover, a viable management of a turbocharging system yields to accomplish an appropriate engine torque for better vehicle drivability [1]. The centripetal turbine, a key component of a turbocharger and linked to a centrifugal compressor by a shaft, recovers partially the engine exhaust gas energy and converts it to a rotational energy to drive the compressor. Then, the compressor forces the extra air into the combustion chamber providing a high boost pressure at the engine intake. The turbocharger turbine stages operate under time fluctuating inlet condition, originated from reciprocating motion of the engine pistons and their head valves closure and opening. Thus, the flow entering the turbine is of a pulsating nature whose form significantly depends on the engine speed, then cylinder number, and displacement. Romagnoli and Martinez-Botas [2] showed a good ability of the meanline as a fast and simple tool for the prediction of turbocharger mixed flow turbines characteristics under steady flow conditions. Ketata and Driss [3] performed a CFD analysis for investigating the flow structure within a turbocharger volute of a mixed flow turbine under various steady flow conditions. Several researchers investigated the effect of the pulsating flow on the turbine performance showing that the turbine unsteady map greatly deviates from its steady characteristic especially at lower pulse frequency [4–11]. In addition, the unsteady character of the turbine has been found sensitive to the pulse frequency [12,13]. Ketata et al. [14] focused on the impact of the wastegate valve opening on the performance of a radial turbine. In another study, Ketata et al. [15] experimentally studied the impact of the

* e-mail: ketata.ahmed.enib@gmail.com

flow frequency on the efficiency of a radial turbine of an automotive turbocharger. The quasi-steady assumption of the turbine presents a major disadvantage that does not take into account the flow dynamics, heat transfer, and mechanical losses depending on the engine condition [16]. Actual 1D-turbine models consist of simplifying the turbine volute geometry to a set of straight and tapered ducts in such a way that the hysteresis mass flow loop becomes close to the real emptying-and-filling phenomenon [12,13,17,18]. However, the rotor has been modeled as a boundary condition based on the steady map of the turbine. One method, proposed by Benson et al. [19], is to model the turbine as either a constant pressure boundary or a variable pressure boundary. Another method is used by Costall [17] and is based on the pressure loss boundary of Benson et al. [19].

This present paper studies the effect of a finite difference scheme on the numerical results of one turbocharger radial turbine operating on a small gasoline engine. Moreover, 1D commercial codes, based on the steady state map, are widely used by the industry for the turbine simulations. However, these codes require performing experiences to obtain the turbine map. To overcome this drawback, the paper suggests a new 1D-meanline coupling method for the turbine steady map building. This code is written in the FORTRAN language and it is based on the unsteady Euler equations. The computed results of the downstream mass flow rate are compared to test data for validation of the calculation method. The turbine performance and flow characteristics are computed and discussed for two engine frequencies using six different finite difference schemes. The results confirm a high unsteadiness of the flow within the turbocharger turbine. In addition, the results show that the choice of the numerical scheme is an important criterion affecting the numerical results accuracy.

2 Test rig description

It is suitable to characterize the turbocharger turbine under pulsating flows from a reciprocating engine exhaust rather than under steady flow conditions. For this end, a test rig of a radial turbocharger turbine is built in the National School of Engineers of Sfax. Figure 1 shows an overview of the test rig. It consists of a turbocharger turbine, embedded to a gasoline four-stroke engine having a cylinder capacity of 1.39 L. The test facility is equipped with an acquisition unit which converts data from the different sensors to numerical ones recognized by the computer. In fact, the acquisition unit is composed of a series of electronic oscilloscopes, for the pressure measurements, and temperature and torque acquisition cards linked to the computer. The turbine and engine speeds are measured with inductive position sensors. All measured unsteady pressures are obtained using piezo-resistive sensors. However, unsteady temperatures are acquired with thermocouples of the type "K".

3 Computational approach

This section provides a brief description of the computational method based on a 1D solution. A code is developed

Fig. 1. Test rig overview.

in our laboratory and written in the FORTRAN language. The turbocharger turbine is considered as a set of duct as proposed by Whitfield et al. [20]. Then, the 1D model includes three pipes: a straight pipe for the inlet duct, a tapered pipe for the volute, and a straight pipe for the exit duct. However, the rotor is modeled as a boundary condition. Figure 2 shows the 1D turbine model as well as the flow chart of the developed FORTRAN solver. The inlet pipe length is 550 mm. The volute pipe of 100 mm of length is taken equal to its mean path distance from the inlet throat area to the cross-section defined by an azimuthal position of 180°. Exit pipe has 300 mm of length. The discretization length is fixedto 10 mm. In this study, two engine speeds are investigated: 3000, and 5000 rpm. These speeds correspond, respectively, to the following frequencies: 83.33 Hz and 50 Hz. The turbine speed is set equal to its time-averaged value of 84476.17 rpm for 50 Hz and of 113870.23 rpm for 83.33 Hz. These values have been obtained from experiments.

The turbine flow can be governed by the Euler formulations in their conservative form, describing a one-dimensional compressible, unsteady, and non-homentropic gas flow [17]. These equations form a non-linear hyperbolic differential equation system as follows:

$$\frac{\partial W}{\partial t} + \frac{\partial F}{\partial x} + C = 0. \quad (2)$$

These governing equations consist of the continuity, momentum and energy equations. In equation (1), W is the state vector of the solution, F is the flux vector, and C is the source term including the effect of heat transfer, area changes, and friction. The conservation law system is commonly arranged in the vector form as follows:

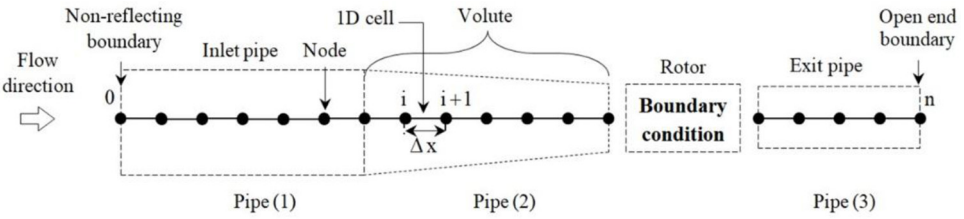

(a)

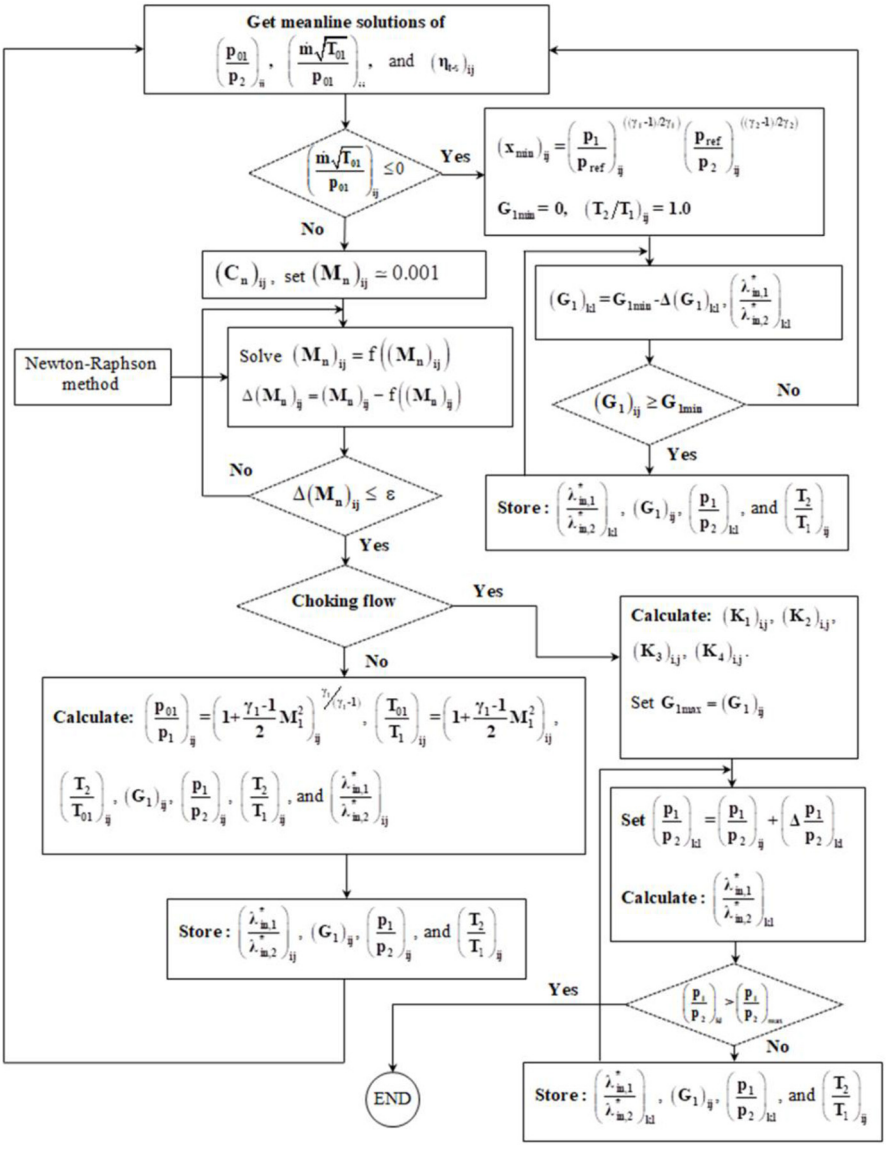

(b)

Fig. 2. A view of (a) the 1D turbine model and (b) the solver flow chart.

$$W = \begin{bmatrix} \rho S \\ \rho u S \\ \rho e_0 S \end{bmatrix}, \quad (2)$$

$$F(W) = \begin{bmatrix} \rho u S \\ \rho(u^2 + p)S \\ \rho u h_0 S \end{bmatrix}, \quad (3)$$

$$C(W) = \begin{bmatrix} 0 \\ -p\dfrac{dS}{dx} \\ 0 \end{bmatrix} + \begin{bmatrix} 0 \\ \rho G S \\ -\rho q S \end{bmatrix}. \quad (4)$$

In this study, four finite difference discretization schemes, which are the Lax-Friedrichs (LF), MacCormack two-step Lax-Wendroff (M2LW), Richtmyer two-step Lax-Wendroff (R2LW), and Modified Richtmyer two-step Lax-Wendroff (MR2LW) methods, have been considered for building the 1D code to simulate the turbocharger turbine. To ensure the convergence of these methods, a Total Variation Diminishing flux limiter (TVD) terms, as proposed by Davis [21], have been introduced in these schemes. More details about these schemes are available in the literature [22].

4 Results and discussion

4.1 Validation

In this study, the distributions of the downstream mass flow rate and the Total-to-Static (TS) efficiency have been plotted for the validation of the numerical model. An FFT filter has been applied to the measured profiles to suppress the existing white noise, coming essentially from the eventual vibration and the surrounding environment of the test rig. Figure 3 compares the predicted results to test data in terms of both the downstream mass flow rate and the TS efficiency at 83.33 Hz of the engine frequency. From these results, it has shown a good match between the predicted results and test data for both the downstream mass flow rate and the TS efficiency over the engine rotation period. Also, it has been observed that the peak values of the mass flow rate and the TS efficiency occur just after the top dead center of each stroke. Figure 4 depicts the computed Mean Absolute Percentage Error (MAPE) for both the TS efficiency and the downstream mass flow rate for one rotation at 83.33 Hz of the engine frequency. From these results, the gap between the predicted and test data is in acceptable range which can confirm a good ability of the developed 1D gas dynamic code to simulate the turbocharger turbine.

The gap between the predicted and test data of the TS efficiency is always greater than that of the downstream mass flow rate for all considered schemes. It is obvious that the accuracy of the efficiency prediction is less sensitive to the choice of the finite-difference scheme compared to that of the mass flow rate. In addition, results showed that the MR2LW finite-difference scheme has led to better accuracy of the mass flow rate and TS efficiency prediction compared to other considered schemes. In fact, minimum values of

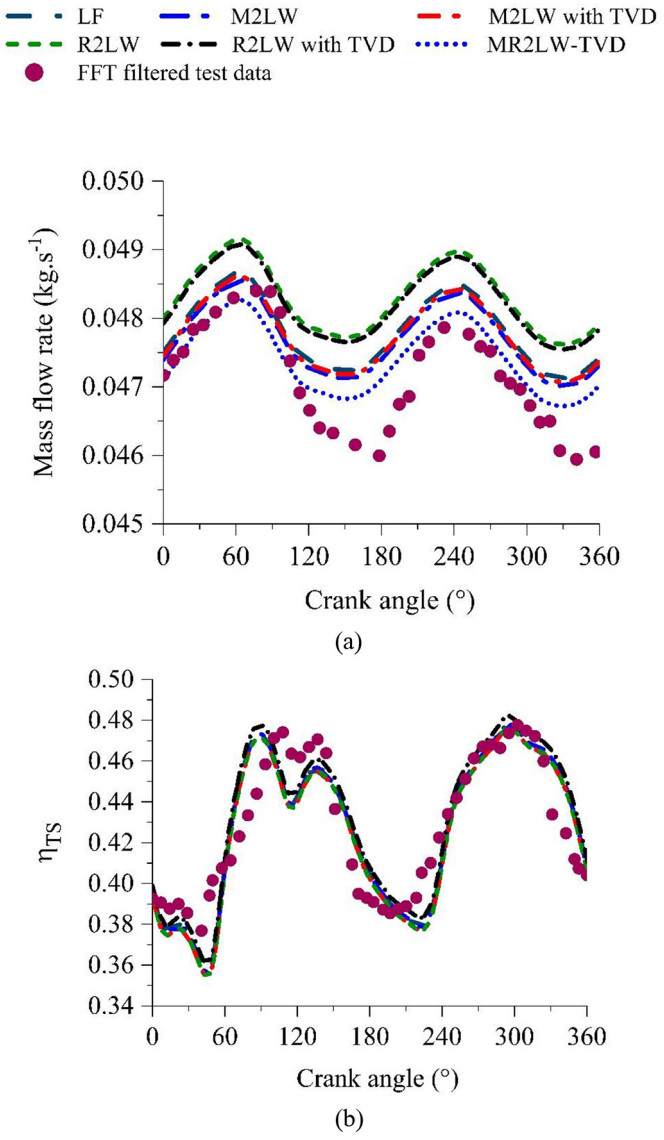

Fig. 3. Comparison of (a) the mass flow rate and (b) the total-to-static efficiency with test data at 83.33 Hz of the engine rotation frequency.

the MAPE of the predicted results, about 0.3% for the downstream mass flow rate and 2.2% for the TS efficiency, have been recorded for the case of the MR2LW finite-difference scheme.

4.2 Steady performance

Figure 5a depicts the distribution of the MFP against the TS expansion ratio and the turbine rotational speed. From these results, it has been noted that the MFP decreases with the rise of the rotational speed. In addition, the reduced mass flow increases with a non-linear slope as the turbine expansion ratio grows. For expansion ratios greater than 2, the reduced mass flow practically stills at the same level. This fact can be explained by an occurring choking flow, in which the Mach number attains its maximum values, at higher expansion ratios. Figure 5b shows the

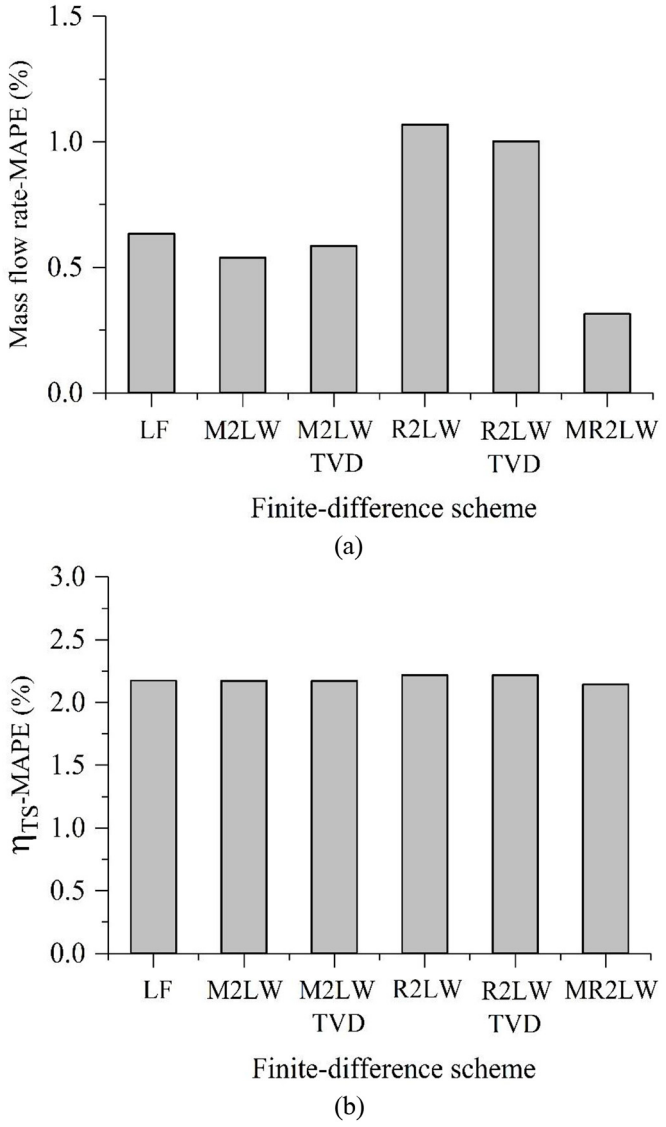

Fig. 4. Mean absolute percentage error of the predicted (a) mass flow rate and (b) total-to-static efficiency at 83.33 Hz of the engine rotation frequency.

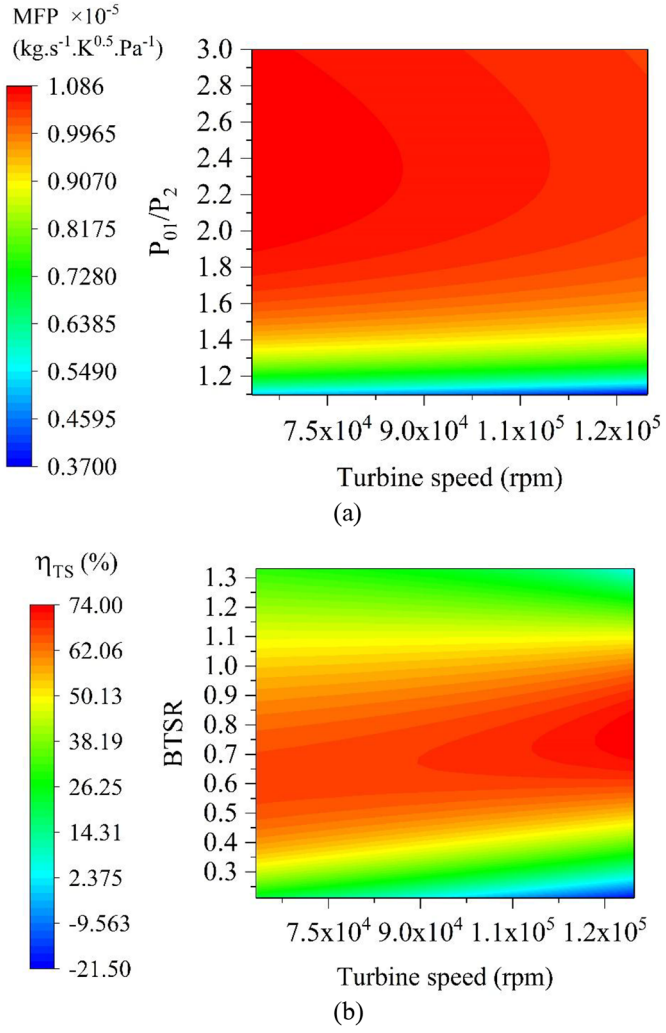

Fig. 5. Distribution of the (a) MFP and (b) total-to-static efficiency from the meanline solution under steady flow conditions.

distribution of the TS efficiency versus the blade tip speed ratio and the rotational speed. From these results, the TS efficiency distribution presents a quasi-hyperbolic shape as a function of the blade tip speed ratio for all considered rotational speeds. The peak TS efficiency occurs at a blade tip speed ratio of 0.7. Close values of the peak efficiency, near to 0.7, have been obtained for the different rotational speeds. With the exception of the optimum operating point, the TS efficiency increases gradually as the rotational speed brings up at weak values of the isentropic velocity.

4.3 Unsteady performance

Figure 6 illustrates the distribution of the MFP against the TS pressure ratio during one engine stroke for the considered numerical schemes. From these results, it has been observed that the MFP presents a hysteresis loop as a function of the TS pressure ratio. This shape can be explained by the mass flow accumulation and discharge phenomenon within the turbine relevant to the pulsating nature of the engine exhaust gas. Moreover, the MFP hysteresis loop, at 50 Hz of the engine frequency, has been found larger than at a frequency of 83.33 Hz. Thus, it can be deduced that the MFP hysteresis loop grows with the decline of the engine frequency. In addition, it has been noted that the MFP prediction is highly sensitive to the numerical scheme. Excepting the MR2LW-TVD scheme, similar shapes of the MFP hysteresis loop have been obtained but, with different values of the MFP. In fact, the MR2LW with TVD leads to an over-prediction of the hysteresis loop compared to other tested schemes. Figure 7 shows the distribution of the turbine TS efficiency against the blade tip speed ratio (BTSR) during one engine stroke for the considered numerical schemes. Also, the TS efficiency presents a hysteresis loop, as a function of the blade tip speed ratio. This hysteresis loop becomes small

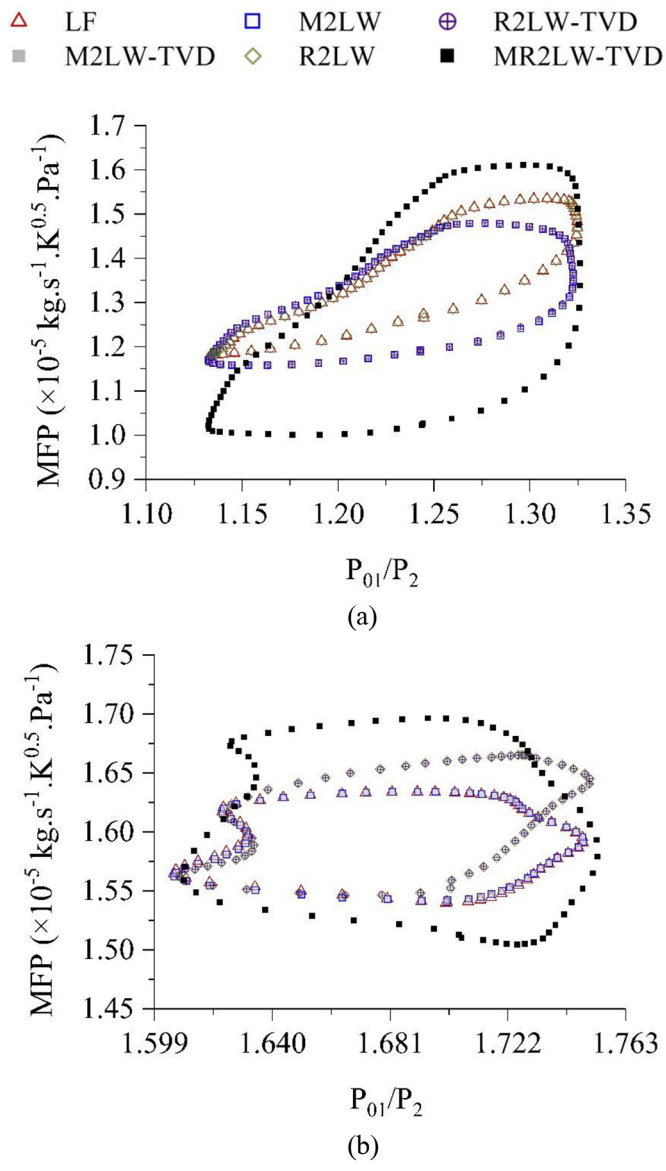

Fig. 6. Unsteady mass flow parameter distributions at (a) 50 Hz and (b) 83.33 Hz of the engine rotation frequency.

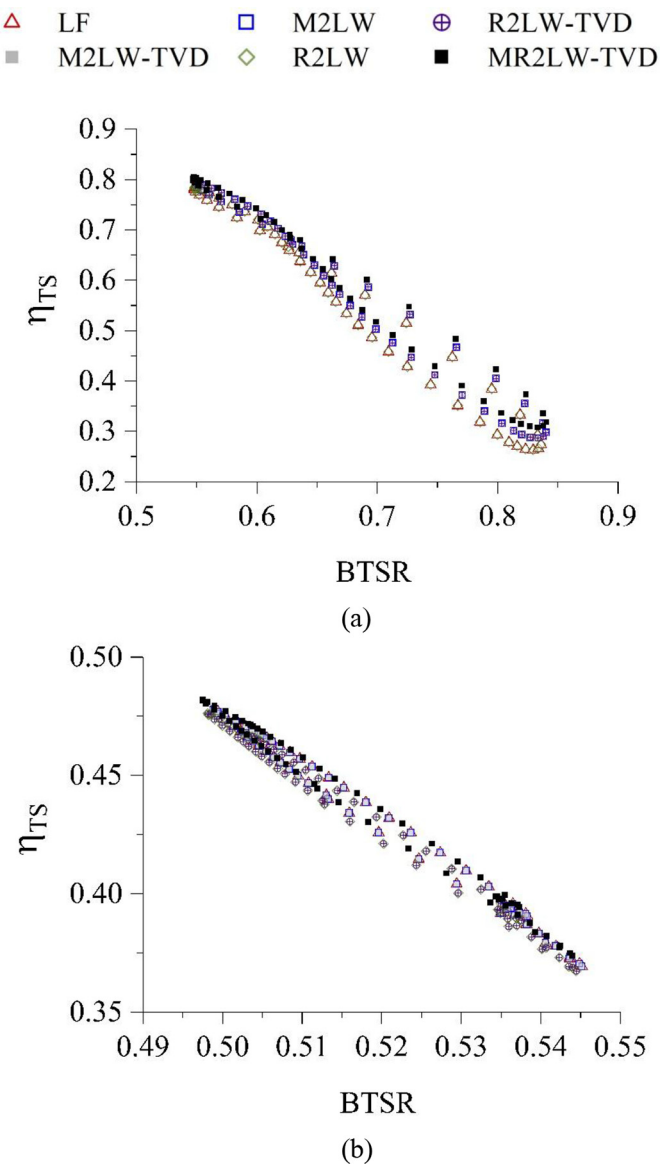

Fig. 7. Unsteady total-to-static efficiency distributions at (a) 50 Hz and (b) 83.33 Hz of the engine rotation frequency.

and fattened with an increasing engine rotation frequency. Maximum values of the TS efficiency characteristic of optimum conditions have been recorded at lower velocity ratios. An increase of the peak efficiency has been observed as the engine frequency decreases from 83.33 Hz to 50 Hz. Thus, the turbocharger turbine is more efficient at lower engine frequencies. The numerical scheme has been found less influential on the efficiency prediction compared to its effect on the MFP estimation. Practically, similar TS efficiency hysteresis loops have been achieved for the different schemes with minor discrepancies. Furthermore, it has been highlighted that the turbine achieves higher blade tip speed ratios when the engine frequency decreases. For example, the maximum blade tip speed ratio is near to 0.85 at a frequency of 50 Hz and it decreases to be near to 0.55 at a frequency of 83.33 Hz. Figure 8 shows the distribution of the actual torque of the turbine shaft against the engine crankshaft angle during one engine rotation for the considered frequencies. The zero degree matches with the top dead center of the first piston. From these results, it is noticeable that the numerical scheme has not a significant effect on the prediction of the turbine torque as similar distributions have been found. Peak torque value occurs just after the combustion and it matches well with the exhaust valve opening of the active cylinder. After the closure of the active exhaust valve, the turbine torque decreases to attain its minimum values. In addition, it is worth noting that the peak torque seems to be insensitive to the engine frequency as similar values have been recorded for both frequency cases. However, the engine frequency influences the minimum torque to be achieved. Its value increases with the growth of the engine frequency. The minimum torque is about 0.015 Nm at a frequency of 83.33 Hz and about 0.0025 Nm at a frequency of 50 Hz. This

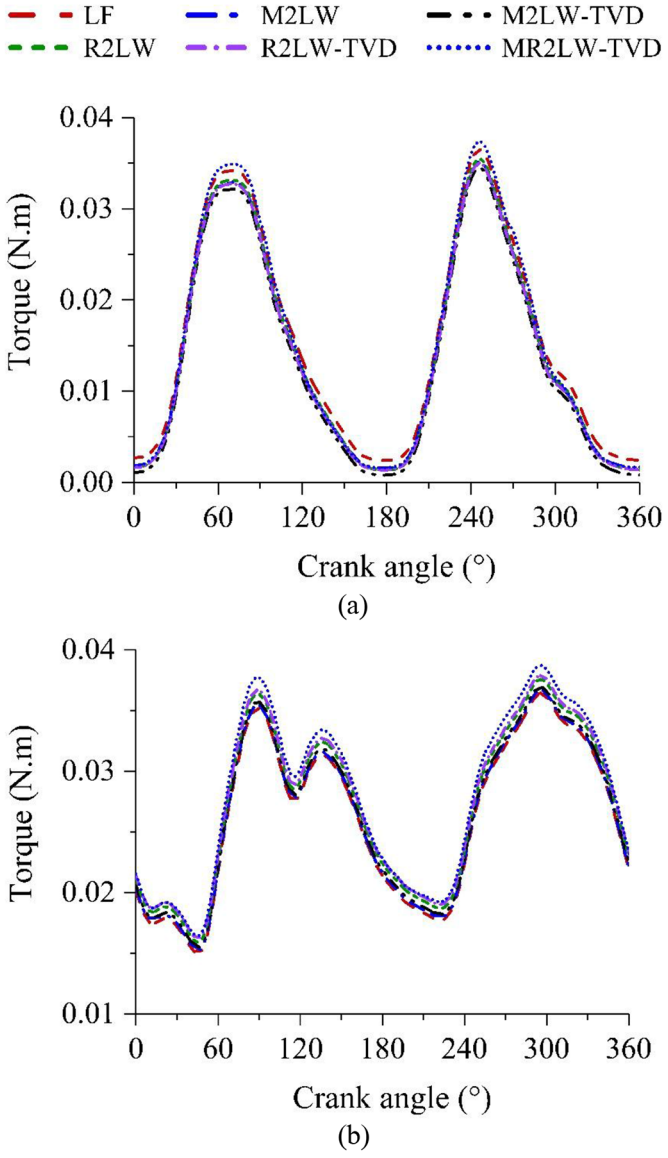

Fig. 8. Unsteady distributions of the torque on the turbine shaft at (a) 50 Hz and (b) 83.33 Hz of the engine rotation frequency.

torque difference due to the frequency change contributes to an eventual lag on the reaction of the turbocharger compressor, related to the turbine through a shaft, during the engine transition from lower to higher engine frequency. Besides, the fluctuating nature of the torque further disturbs the rotation of the compressor wheel by creating a discontinuity in the time of the air compression process.

5 Conclusion

In this paper, the unsteady behavior of a turbocharger radial turbine, operating on a small gasoline four-stroke engine, was investigated with a developed 1D gas dynamic code, written in the FORTRAN language. The 1D numerical solutions, based on the turbine steady map, are carried out for six different finite difference methods. A new 1D-meanline method is proposed to build the turbine steady map instead of performing tests for the turbine boundary treatment. The turbine is tested for two frequencies of 50 Hz and 83.33 Hz with a developed test rig in the National School of Engineers of Sfax. The comparison between the computed and experimental results showed a good agreement for the different finite-difference schemes. This result ensures the validity of the developed code for turbocharger turbines gas dynamic simulations. In addition, the results showed that the MR2LW scheme has led to minimum deviations of the predicted performance results to test data. The results proved a mass flow accumulation and discharge phenomenon within the turbine. This phenomenon has led to a significant deviation of the distribution of the unsteady total to static efficiency and mass flow parameter from their steady-state ones. In fact, both mass flow parameter and TS efficiency present a hysteresis loop as a function of the total to static pressure ratio and the blade tip speed ratio, respectively. These hysteresis loops become larger as the engine frequency decreases. The numerical scheme is significantly influential on the distribution of the turbine mass flow parameter and efficiency. The torque considerably decreases with the decline of the engine speed. This fact may disturb the compressor wheel, driven by the turbine shaft.

Nomenclature

C	Source term, or rotor boundary constant
e_0	Stagnation internal energy
F	Flux vector
MFP	Mass flow parameter ($\mathrm{kg\,s^{-1}\ \sqrt{K}\ Pa^{-1}}$)
S	Area ($\mathrm{m^2}$)
t	Time (s)
u	Velocity ($\mathrm{m.s^{-1}}$)
W	State vector
η_{TS}	Total-to-static efficiency (dimensionless)
ρ	Density ($\mathrm{kg.m^{-3}}$)
Δt	Time step (s)
Δx	Spatial discretization length (m)

Subscript

0	Stagnation point
1	Turbine inlet
2	Turbine outlet
TS	Total-to-Static

Abbreviation

BTSR	Blade tip speed ratio
CFD	Computational fluid dynamics
EGR	Exhaust gas recirculation
FFT	Fast fourier transform
LF	Lax-Friedrichs
MAPE	Mean absolute percentage error
M2LW	MacCormack second order Lax-Wendroff
MR2LW	Modified Richtmyer second order Lax-Wendroff
R2LW	Richtmyer second order Lax-Wendroff
TVD	Total variation diminishing

References

[1] D. Petitjean, L. Bernardini, C. Middlemass, S. Shahed, Advanced gasoline engine turbocharging technology for fuel economy improvements. SAE Technical Paper, 2004

[2] A. Romagnoli, R. Martinez-Botas, Performance prediction of a nozzled and nozzleless mixed-flow turbine in steady conditions, Int. J. Mech. Sci. **53**, 557–574 (2011)

[3] A. Ketata, Z. Driss, CFD techniques and energy applications, in: Numerical investigation for a vanned mixed flow turbine volute under steady conditions, Springer International Publishing, New York, 2018

[4] N. Baines, Turbocharger turbine pulse flow performance and modelling 25 years on, *9th IMechE International Conference on Turbochargers and Turbocharging, London, May 19–20*, 2010

[5] R. Benson, A. Whitfield, An experimental investigation of the non-steady flow characteristics of a centrifugal compressor, Proc. Inst. Mech. Eng. **180**, 641–672 (1965)

[6] R.S. Benson, Nonsteady flow in a turbocharger nozzleless radial gas turbine. SAE Technical Paper, 1974

[7] M. Capobianco, S. Marelli, Experimental investigation into the pulsating flow performance of a turbocharger turbine in the closed and open waste-gate region, 9th International Conference on Turbochargers and Turbocharging, London, 2010

[8] A. Dale, N. Watson, Vaneless radial turbocharger turbine performance, Proceedings of the Institution of Mechanical Engineers, 3rd International Conference on Turbocharging and Turbochargers, Paper (C110/86), 1986

[9] S. Szymko, R. Martinez-Botas, K. Pullen, Experimental evaluation of turbocharger turbine performance under pulsating flow conditions, ASME Paper No. GT2005-68878, 2005

[10] D. Winterbone, B. Nikpour, G. Alexander, Measurement of the performance of a radial inflow turbine in conditional steady and unsteady flow, Proceedings of the 4th International Conference on Turbocharging and Turbochargers, May, 1990, London, pp. 22–24

[11] N. Karamanis, R. Martinez-Botas, Mixed-flow turbines for automotive turbochargers: steady and unsteady performance, Int. J. Engine Res. **3**, 127–138 (2002)

[12] A. Costall, R.F. Martinez-Botas, Fundamental characterization of turbocharger turbine unsteady flow behavior, ASME Paper No. GT2007–28317, 2007

[13] M. Chiong, S. Rajoo, R. Martinez-Botas, A. Costall, Engine turbocharger performance prediction: One-dimensional modeling of a twin entry turbine, Energy Convers. Manag. **57**, 68–78 (2012)

[14] A. Ketata, Z. Driss, M.S. Abid, Impact of the wastegate opening on radial turbine performance under steady and pulsating flow conditions, Proc. Inst. Mech. Eng., Part D J. Automobile Eng. (2019) https://doi.org/10.1177/0954407019852494

[15] A. Ketata, Z. Driss, M.S. Abid, Experimental analysis for performance evaluation and unsteadiness quantification for one turbocharger vane-less radial turbine operating on a gasoline engine, Engineering **43**, 4763–4781 (2018)

[16] M. Nakhjiri, P.F. Pelz, B. Matyschok, L. Däubler, A. Horn, Apparent and real efficiency of turbochargers under influence of heat flow, 14th International Symposium on Transport Phenomena and Dynamics of Rotating Machinery (ISROMAC-14), Honolulu, HI, February, 2012

[17] A. Costall, A one-dimensional study of unsteady wave propagation in turbocharger turbines, 2008

[18] A. Costall, S. Szymko, R.F. Martinez-Botas, D. Filsinger, D. Ninkovic, Assessment of unsteady behavior in turbocharger turbines, ASME Paper No. GT2006-90348, 2006

[19] R.S. Benson, J.H. Horlock, R.S.R.S. Benson, D.E. Winterbone, The thermodynamics and gas dynamics of internal-combustion engines, Clarendon Press, New York, 1982

[20] A. Whitfield, N.C. Baines, Design of radial turbomachines, 1990

[21] S.F. Davis, TVD finite difference schemes and artificial viscosity, 1984

[22] R.J. LeVeque, Numerical methods for conservation laws, Birkhäuser, Basel, 1992

Cite this article as: A. Ketata, Z. Driss, M.S. Abid, 1D gas dynamic code for performance prediction of one turbocharger radial turbine with different finite difference schemes, Mechanics & Industry **20**, 627 (2019)